

MOL #55434

KLYP956 is a Non-Imidazole-Based Orally Active Inhibitor of Nitric Oxide Synthase Dimerization

Kent T. Symons, Mark E. Massari, Phan M. Nguyen, Tom T. Lee, Jeffrey Roppe, Céline Bonnefous, Joseph E. Payne, Nicholas D. Smith, Stewart A. Noble, Marciano Sablad, Natasha Rozenkrants, Yan Zhang, Tadimeti S. Rao, Andrew K. Shiau and Christian A. Hassig

Kalypsys Department of Biology: KTS, MEM, PMN, TTL, AKS, CAH

Kalypsys Department of Chemistry: JR, CB, JEP, NDS, SAN

Kalypsys Department of Pharmacology: MS, NR, YZ, TSR

Kalypsys, Inc., 10420 Wateridge Circle, San Diego, CA 92121, USA

Department of Molecular Biology, The Scripps Research Institute, 10550 N. Torrey Pines Road, La Jolla, CA 92037, USA: CAH

MOL #55434

Running Title: Novel Nitric Oxide Synthase Dimerization Inhibitor

Corresponding author: Christian A. Hassig

Address/Affiliations:

Kalypsys, Inc.
10420 Wateridge Circle
San Diego, CA 92121 USA

The Scripps Research Institute
10550 N. Torrey Pines Road
La Jolla, CA 92037 USA

858-431-6331 (ph)
858-754-3301 (fax)
hassig@scripps.edu

Pages of Text: 36
of Tables: 3
of Figures: 8
of References: 31
of Words in Abstract: 202
 Introduction: 529
 Discussion: 1161

Nonstandard Abbreviations:

NO, nitric oxide; NOS, nitric oxide synthase; iNOS, inducible nitric oxide synthase; nNOS, neuronal nitric oxide synthase; eNOS, endothelial nitric oxide synthase; DAN, 2,3-diaminonaphthalene; LPS, lipopolysaccharide; PEG, polyethylene glycol; LT SDS-PAGE, low temperature sodium dodecylsulfate-polyacrylamide gel electrophoresis; SEITU, S-ethylisothiourea; BBS-4, (R)-1-(2-(1H-imidazol-1-yl)-6-methylpyrimidin-4-yl)-N-(2-(benzo[d][1,3]dioxol-5-yl)ethyl)pyrrolidine-2-carboxamide; IFN- γ , gamma interferon; IL1- β , interleukin 1 beta; TNF- α , tumor necrosis factor alpha; ADMET, absorption distribution metabolism excretion toxicology; BH₄, tetrahydrobiopterin; DTT, dithiothreitol; DI, dimerization inhibitor; 1400W, [N-(3-aminoethyl)benzyl]-acetamidine hydrochloride

MOL #55434

Abstract

Nitric oxide synthases (NOS) generate nitric oxide (NO) through the oxidation of L-arginine. Inappropriate or excessive production of NO by NOS is associated with the pathophysiology of various disease states. Efforts to treat these disorders by developing arginine mimetic, substrate-competitive NOS inhibitors as drugs have met with little success. Small molecule mediated inhibition of NOS dimerization represents an intriguing alternative to substrate-competitive inhibition. An ultra high-throughput cell-based screen of 880,000 small molecules identified a novel quinolinone with inducible NOS (iNOS) inhibitory activity. Exploratory chemistry based on this initial screening hit resulted in the synthesis of KLYP956, which inhibits iNOS at low nanomolar concentrations. The iNOS inhibitory potency of KLYP956 is insensitive to changes in concentrations of the substrate arginine, or the cofactor tetrahydrobiopterin. Mechanistic analysis suggests that KLYP956 binds the oxygenase domain in the vicinity of the active site heme and inhibits iNOS and neuronal NOS (nNOS) by preventing the formation of enzymatically active dimers. Oral administration of KLYP956 inhibits iNOS activity in a murine model of endotoxemia and blocks pain behaviors in a formalin model of nociception. KLYP956 thus represents the first non-imidazole-based inhibitor of iNOS and nNOS dimerization and provides a novel pharmaceutical alternative to previously described substrate competitive inhibitors.

MOL #55434

Introduction

The overproduction of nitric oxide (NO) has been implicated in the pathophysiology of a broad range of human diseases including pain, inflammation, migraine and neurodegenerative disorders. Three nitric oxide synthase (NOS) isoforms have been described, including endothelial (eNOS), neuronal (nNOS) and inducible (iNOS). Data support the notion that the inhibition of iNOS and nNOS may have therapeutic utility in the treatment of a variety of disease states including inflammation and pain. However, inhibition of eNOS is considered detrimental as it results in elevated systemic blood pressure. Among the three isoforms, iNOS generates stoichiometrically higher amounts of NO and is expressed at sites of inflammation. Irrespective of the source, excessive NO can generate peroxynitrite and other reactive species that can trigger protein nitrosylation leading to tissue damage (Vallance and Leiper, 2002).

NOS isoforms catalyze the NADPH and O₂ – dependent oxidation of L-arginine to NO and citrulline, with N-hydroxy-L-arginine formed as an intermediate. NOS isoforms are flavoheme enzymes that are only active as homodimers. Each monomer has a carboxy-terminal diflavin-reductase domain and an amino-terminal oxygenase domain. Extensive studies have defined many biochemical and structural requirements for NOS dimerization. Dimerization is thought to activate the enzyme by sequestering iron, generating high-affinity binding sites for arginine and the essential cofactor tetrahydrobiopterin (BH₄), and allowing electron transfer from the reductase-domain flavins of one monomer to the oxygenase-domain heme of the other monomer (Siddhanta et al., 1998). Several reports have suggested that both iNOS and nNOS activity is

MOL #55434

regulated by controlling the timing and extent of dimer formation and/or stability via protein interactions and NO itself (Kone et al., 2003;Li et al., 2006).

Small-molecule inhibitors of NOS have been described and appear to function through two predominant modes of action. Many classical substrate-competitive inhibitors share structural similarities with L-arginine, and thus are sensitive to local arginine concentrations. These compounds often have isoform selectivity limitations and may also interfere with physiological processes intimately dependent on arginine transport and metabolism (Paige and Jaffrey, 2007;Robertson et al., 1993;Edwards et al., 1998;Olken et al., 1994;Feldman et al., 1993). More recently, several groups have described small molecules capable of interfering with the formation and enzymatic activity of NOS dimers. With the exception of a peptide-derived compound (Chida et al., 2005), all iNOS dimerization inhibitors described to date contain an N-substituted imidazole moiety that is thought to directly coordinate the heme iron in the active site of the enzyme (Ohtsuka et al., 2002;McMillan et al., 2000;Sohn et al., 2008;Sennequier et al., 1999). Given that non-substrate mimetic inhibitors, such as those that act by blocking formation of the enzymatically active dimer, are likely to have distinct *in vivo* profiles, we conducted a cell-based high-throughput screen of approximately 880,000 small molecules to discover novel, non-arginine, non-imidazole-based inhibitors of recombinant human iNOS. These efforts resulted in the identification of a quinolinone scaffold that was subsequently optimized for potency and selectivity to generate KLYP956, a low nanomolar inhibitor of iNOS with greater than 1900-fold selectivity over eNOS. Mechanistic analysis suggests that KLYP956 acts by preventing the formation of the stable enzymatically active form of iNOS and nNOS. Spectral studies suggest

MOL #55434

that the compound binds to the enzyme in a mode distinct from that of the N-substituted imidazole-based inhibitors.

Materials and Methods

Compounds

S-ethyl isothiurea (SEITU) and 1400W were obtained from Sigma, BBS-4 and KLYP956 were synthesized internally at Kalypsys, Inc.

Molecular Cloning

Using standard PCR techniques, full-length coding sequences were generated to match the following published accession numbers: human iNOS (NM_000625), human nNOS (NM_000620), human eNOS (NM_000603), murine iNOS (NM_010927), murine nNOS (NM_008712) and murine eNOS (NM_008713). All clones were sequenced to confirm identity. Full-length coding sequences were subcloned into pCS2 mammalian expression constructs (described in <http://sitemaker.umich.edu/dlturner.vectors/home>).

Cell Culture

A172 human glioblastoma, RAW 264.7 murine macrophage, and HEK293 cells (ATCC) were cultured in DMEM containing 10% FBS, 100 U/ml penicillin, and 100 µg/ml streptomycin. HEK293 human nNOS stable cells were grown in the media above supplemented with 2 µg/ml puromycin to retain selection. A172 cells were stimulated to express iNOS by adding a cocktail containing hIFN-γ (4,000 U/ml), hTNF-α (40 ng/ml), hIL-1β (4 ng/ml) (Roche Diagnostics).

MOL #55434

RAW 264.7 cells were stimulated in media with lipopolysacharride (1 $\mu\text{g/ml}$) (Sigma) and mIFN- γ (100 U/ml) (Roche Diagnostics). HEK 293 cells were transiently transfected with a CMV-driven plasmid expressing murine iNOS, murine nNOS, murine eNOS, human iNOS, human nNOS, or human eNOS.

Nitric Oxide Detection (DAN Assay)

HEK293 cells were plated into 15 cm dishes and grown to 70% confluency. Cells were transiently transfected with 30 μl Fugene and 10 $\mu\text{g/dish}$ of the appropriate NOS plasmid for 4 hours. Transfected cells were plated in 384- or 1536-well plates at a density of 5×10^5 cells/ml and compounds were added immediately using a proprietary pin-transfer technology. Cells for the iNOS assay were incubated for 18 hours for nitrite accumulation. NO production was determined indirectly by measuring nitrite accumulation in cell culture supernatants using the 2,3-diaminonaphthalene (DAN) assay. Supernatants were mixed with (DAN 10 $\mu\text{g/ml}$ final; Invitrogen) diluted in DMEM supplemented with hydrochloric acid (0.1N final) and incubated for 20 minutes at room temperature. Fluorescence (excitation 360 nm/ emission 425 nm) was measured after increasing pH with sodium hydroxide (0.12N final) on an Acquest plate reader (Molecular Devices). Cells for eNOS and nNOS were incubated 24 hours with compound and then activated by ionophore (0.8 μM final A23187 for eNOS or 30 μM final ionomycin for nNOS) and incubated an additional 18 hours for nitrite accumulation followed by the DAN assay.

Biochemical Inhibition of iNOS and nNOS in the Arginine to Citrulline Conversion Assay

MOL #55434

HEK293 cells were plated into 15 cm dishes and grown to 70% confluency. Cells were transiently transfected with 10 μ g/dish of human iNOS or nNOS expression plasmid for 24 hours. Proteins were harvested with 1 ml of 1 mM EDTA, centrifuged 2 minutes at 400g, and lysed with 0.1% Triton-X-100 in 50 mM potassium phosphate buffer containing protease inhibitors (Roche). Lysates were then incubated with compound for 20 minutes. Reaction mix (Stratagene NOS Detect) was added containing 14 C- labeled arginine (GE Healthcare). Conversion of arginine to citrulline was determined by ion-exchange separation and scintillation counting.

Arginine Competition

HEK293 cells were plated into 15 cm dishes and grown to 70% confluency. Cells were transiently transfected with 30 μ l Fugene and 10 μ g/dish of human iNOS expression plasmid for 3 hours. Media was replaced with arginine-free DMEM containing 0.3% BSA for 1 hour. Cells were trypsinized, diluted to 5×10^5 cells/ml in either 10 μ M or 1000 μ M arginine in DMEM containing 0.3% BSA and 5 μ l/well was plated into a black 1536-well plate. Compounds were added and cells were incubated for 18 hours followed by the DAN assay as described above.

BH₄ Competition

A172 cells (4×10^6 cells/well) were seeded in a 384-well plate for 4 hours. Sepiapterin (Cayman) was added to yield a final concentration of 0 μ M, 1 μ M, or 10 μ M diluted in induction cocktail (see cell culture) and were incubated for 22 hours followed by the DAN assay as described above.

MOL #55434

iNOS_{oxy} Spectral Shift

The sequence encoding human iNOS_{oxy} (amino acids 74-504) was inserted into pET29a(+). The resulting construct carrying a C-terminal 6×His tag was expressed in *E. coli* and purified by Ni-NTA IMAC followed by Mono Q IEC. To generate monomeric human iNOS_{oxy}, a protocol was used as described previously (Sennequier et al., 1999). Briefly, protein was diluted in 5M urea for 1.5 hours, then dialyzed against 2M urea for 4 hours, followed by 0.1M urea overnight. Protein was diluted in spectral shift buffer (25 mM HEPES, 5% glycerol, 1 mM DTT) during urea treatment, as well as, during the spectral shift assay. All incubations were at 4 °C. For spectral scans, 50 µl of 0.3 mg/ml of urea-treated protein was dispensed into a 384-well assay dish in 25 mM HEPES, 5% glycerol, 1 mM DTT. 500 nl of compound was added via the proprietary Kalypsys pin-based transfer technology and incubated for 30 minutes at room temperature. A spectral scan (UV-Vis) was measured using a Spectramax Plus spectrophotometer (Molecular Devices).

Gel-based dimer assay (Low Temperature SDS-PAGE) for iNOS and nNOS

RAW 264.7 cells were seeded into 6-well dishes at a density of 1.5×10^6 cells/well. Cells were incubated for 5 hours and 1 mL of media was removed from each well and replaced with 1 mL of a 2X cocktail containing mIFN- γ (100 U/mL final), LPS (2 µg/mL final) and compound or vehicle (0.1% DMSO final) diluted in DMEM with 10% serum. Cells were incubated overnight at 37 °C, 5% CO₂. Cells were washed once with ice cold PBS and then 200 µL of ice-cold lysis buffer (250 mM sucrose, 10 mM Tris pH 7.5, 1 mM EDTA) containing protease inhibitors was added to each well. Cells were scraped from the dish and transferred to micro-centrifuge tubes on ice. Samples were sonicated for 5 seconds at setting 4 (Branson) and centrifuged at 16,000g

MOL #55434

for 10 minutes at 4 °C. The concentration of protein was normalized using a Bradford assay (Advanced). An equal volume of ice-cold 2X loading buffer (63mM Tris pH 6.8, 10% glycerol, 3% SDS, 1% β -mercaptoethanol, 0.002% Bromophenyl Blue) was added to each sample and loaded onto a 4-20% Tris-glycine polyacrylamide gel (Invitrogen). The gel was run in pre-chilled 1X SDS running buffer in a cold room for 2.5 hours at 125 V. Proteins were transferred to nitrocellulose for 2.5 hours at 70 V in 1X transfer buffer and detected as per methods described below (Western blotting).

FLAG Co-Immunoprecipitation HA detection and Biochemical Disruption

The N-terminus of human iNOS was tagged with either influenza (HA) hemagglutinin peptide (YPYDVPDYA) or FLAG peptide (DYKDDDDK) and linked to iNOS via two glycine residues using insertion mutagenesis following the protocol described previously (Wang and Malcolm, 1999). HEK293 cells were cotransfected with HA-tagged and FLAG-tagged human iNOS for four hours followed by addition of compound and incubation overnight (No compound was added to the cotransfected cells for the biochemical disruption assay.) Prior to harvesting cells, 50 μ l of media from each well was plated in quadruplicate for NO determination via the DAN assay. Cells were harvested with 1 mL of ice cold PBS, centrifuged 2 minutes at 400 x g and washed once with 1 mL of ice-cold PBS. Cells were lysed with 500 μ l lysis buffer (25 mM Tris pH 8.0, 10% glycerol, 150 mM NaCl and 0.5% Triton-X-100) containing protease inhibitors. Extracts were centrifuged at 16,000 x g for 10 minutes at 4 °C. The concentration of protein was normalized using a Bradford assay (Advanced). Approximately 200 to 400 μ g of protein was immunoprecipitated for 1 hour at 4 °C using anti-FLAG M2 beads (Sigma) in 1 mL (for biochemical disruption of dimers, compound was added to lysates one hour prior to the M2

MOL #55434

immunoprecipitation). Immunoprecipitates were washed three times with 1 mL of lysis buffer followed by elution with 50 μ l of 2x NuPage loading buffer. DTT was added to each sample at a final concentration of 0.1 M and samples were loaded onto a 4-12% Bis-Tris polyacrylamide gel (Invitrogen). The gels were run in 1X MES running buffer for 1 hour at 160 V. Proteins were transferred to nitrocellulose for 2 hours at 80 V in 1X transfer buffer and probed as described below (Western blotting).

Western Blotting

Membranes were blocked overnight in Blotto - 20 mM Tris pH 8.0, 150 mM NaCl, 0.05% (v/v) Tween-20 (TBST) containing 3% (w/v) nonfat milk at 4 °C. The membranes were incubated in 1:2,500 of mouse anti-iNOS (BD Biosciences), 1:1,000 of mouse anti-Flu 16B12 (Covance), 1:2,500 of mouse anti-nNOS (BD Biosciences), or 1:4,000 of rabbit anti-calmodulin (Abcam) in Blotto for 1 hour at room temperature followed by 3 x 5 minute washes in TBST. The blot was then incubated in a 1:2,000 dilution of goat anti-mouse (BioRad) or 1:5,000 of goat anti-rabbit (Santa Cruz) HRP-conjugated secondary antibody in Blotto for 1 hour at room temperature. Following 4 x 5 minute washes, the proteins were visualized by chemiluminescence using SuperSignal West Dura (Pierce) detection reagent and captured on a CCD-based imaging device (Alpha Inotech).

Mouse LPS Model

Male Balb/C mice were given intraperitoneal injection of LPS solution in saline (Sigma, L2880, dose: 10 mg/kg). Blood samples were collected under isofluorane anesthesia at pre-determined time points for analysis of nitrates (6 hr post-LPS). KLYP956 was administered by oral gavage

MOL #55434

immediately before LPS injection. Plasma samples were allowed to thaw in ice and filtered through a 10 KDa molecular weight cut-off filter (MultiScreen Filter Plate; Ultracel-10 Membrane, Fisher Scientific, cat#MAUF01010), at 2000 x g for 10 minutes at 4°C. Plasma nitrates, a marker of iNOS activity, were measured using a fluorimetric assay kit (Cayman Chemicals, Ann Arbor, MI) following the formation of a fluorophore by the addition of 2,3-diaminonaphthalne (DAN). Fluorescence was measured using the Aquest plate reader (Molecular Devices). All results are expressed as mean + SEM.

Mouse Formalin Model

Compounds was administered to animals via oral gavage in a vehicle consisting of 9: 0.5: 0.5: 90 of PEG-400: Tween-80: PVP-K30: Cm-cellulose in water (0.5% w/v) 1 hour prior to formalin challenge. For intraperitoneal dosing the vehicle composition was 9: 0.5: 0.5: 90 of PEG-400: Tween-80: PVP-K30: water and the compounds were administered 1 hour prior to formalin challenge. The formalin solution for intraplantar injection was first prepared by diluting a 10% formalin stock solution to 5% final with 0.9% saline. A volume of 20 μ L was injected into the left hind paw of each animal.

Immediately after injection of formalin, mice were placed in a see-through observation chamber (Kalypsys, Inc.) and a timer was activated. The duration of pain behaviors (hind paw flinches, licking and biting) displayed by the injured hind paw was counted in 5 minute intervals. Phase I was observed from 0-5 minutes post-formalin injection. Phase II was observed from 25-45 minutes post-formalin injection. Data are presented as time spent in nociceptive behaviors during Phase I (0-5 minutes post-formalin) and Phase II (25-45 minutes post-formalin). There was a single observer throughout the study, and observers were not blinded with respect to

MOL #55434

treatment group. All in vivo experiments were conducted in accordance with the Guide for the Care and Use of Laboratory Animals and promulgated by the N.I.H.

Results

High-Throughput Screening Identifies a Novel Potent iNOS Inhibitor

In an effort to identify non-imidazole based inhibitors of iNOS, we conducted a homogeneous cell-based high-throughput screen (HTS) of 880,000 small molecules for inhibitors of recombinant human iNOS. A series of secondary assays were implemented in a matrix fashion to select for direct, non-substrate competitive, inhibitors of human iNOS with favorable pharmaceutical properties. One compound that emerged from this screening paradigm displayed favorable potency and isoform selectivity, as well as good preliminary ADMET properties (data not shown). Exploratory chemistry efforts led to the synthesis of KLYP956, a highly potent quinolinone-based human iNOS inhibitor that neither shares structural similarity to arginine-based inhibitors (such as SEITU) nor to N-substituted imidazole-based inhibitors (such as BBS-4) (Fig. 1A, 1B). Given the novel chemical structure of KLYP956, a series of studies were conducted to characterize its selectivity properties as well as to investigate the mechanism of NOS inhibition.

KLYP956 Inhibits iNOS and nNOS in Cells but not in Reconstituted Biochemical Assays

While the inhibitory activity of the high throughput screening leads against recombinant human iNOS was robust, inhibition of the murine iNOS enzyme was surprisingly poor, with an $IC_{50} > 50$ μ M (data not shown). However, the improved potency of KLYP956 against human iNOS was

MOL #55434

paralleled by improved potency against murine iNOS. In cell-based assays, KLYP956 inhibits both human and murine iNOS activity in a concentration-dependent manner with IC₅₀ values of 0.01 μM and 0.14 μM, respectively (Fig. 2A and Table 1). Next, we investigated the isoform and species selectivity profile of KLYP956. The compound inhibits human nNOS and human eNOS, but requires significantly higher concentrations than those necessary to inhibit iNOS, with IC₅₀ values of 2.6 μM and 19.0 μM, respectively. Consequently, in humans, the selectivity of KLYP956 for iNOS over nNOS is 260-fold and that over eNOS is 1,900-fold (Table 1).

Surprisingly, in addition to an approximate 10-fold difference in potency between human and murine iNOS, an inverse potency relationship is seen for human versus murine nNOS.

KLYP956 is essentially equipotent on murine iNOS and murine nNOS (Table 1).

The majority of substrate competitive iNOS inhibitors exhibit high potency in biochemical assays, but are considerably less potent in cell-based assays. In contrast, imidazole-based dimerization inhibitors such as BBS-4 display an opposite profile, being substantially more potent in cell-based assays (Davey et al., 2007; Blasko et al., 2002). As seen in Figures 2B and 2C, BBS-4 and KLYP956 display limited inhibition against human iNOS and human nNOS in the biochemical inhibition assay, even at the highest concentration tested (30 μM). In contrast, the non-selective arginine mimetic, SEITU, potently inhibits both NOS isoforms *in vitro* (Fig. 2B and Fig. 2C).

To characterize the biochemical mechanism by which KLYP956 inhibits NOS, we then tested the effects of changes in substrate concentration on KLYP956 as compared to previously reported NOS inhibitors. Substrate competitive NOS inhibitors display significant shifts in IC₅₀ values as a consequence of elevated arginine concentrations. For example, SEITU and 1400W display a 15-fold and 9-fold potency shift when the arginine concentration in cell culture media

MOL #55434

is increased from 10 μ M to 1 mM, respectively (Table 2). Consistent with the *in vitro* biochemical inhibition data described above, KLYP956 and BBS-4 display little if any significant change in potency when arginine concentrations in cell culture media are modulated by two orders of magnitude (Table 2).

Similarly, changes in the concentration of the essential cofactor tetrahydrobiopterin (BH₄) can potentially affect the potency of compounds if they are competitive with BH₄. This possibility can be investigated by supplementing excess sepiapterin, a biopterin precursor, into cell-based inhibition assays (Blasko et al., 2002). To test whether KLYP956 inhibits BH₄ binding, we determined KLYP956-mediated cellular iNOS inhibition with varying concentrations of sepiapterin, ranging from 0 μ M to 10 μ M. Under the conditions tested, the potency of neither KLYP956, nor BBS-4, was perturbed by changes in sepiapterin concentrations, indicating that KLYP956 is unlikely to be competitive with BH₄ (Table 3).

KLYP956 Perturbs iNOS_{oxy} Domain Heme Spectrum in a Distinct Mode from Imidazole-based Inhibitors

Direct interaction with the iNOS oxygenase (iNOS_{oxy}) domain can be detected spectrophotometrically by measuring changes in the heme absorbance spectrum of the purified enzyme (McMillan and Masters, 1993; Sennequier and Stuehr, 1996). Bacterially-expressed six-histidine tagged human iNOS_{oxy} domain was purified and partially denatured to yield a population of monomeric and loose dimeric enzyme that, in the presence of DTT, displays a characteristic split Soret absorbance peak at 378 nm and 460 nm (Fig. 3). The addition of KLYP956 (1 μ M to 10 μ M) results in a concentration-dependent shift in the absorbance spectrum, generating a single Soret maximum at 396 nm (Fig. 3). A similar spectral shift has

MOL #55434

been described when the enzyme is coincubated with arginine and BH₄ (Sennequier et al., 1999). This spectral shift contrasts sharply with that generated by imidazole-based compounds that produce a single Soret peak centered at 429 nm, indicating a shift in the heme iron to the low spin state (Blasko et al., 2002).

KLYP956 Destabilizes Both Murine and Human iNOS Dimer in Cells

The quaternary structural status of iNOS isolated from activated murine macrophages can be visualized using partially denaturing low-temperature SDS-PAGE followed by immunoblotting with antibodies recognizing the iNOS protein. Under these experimental conditions, a sub-population of untreated or vehicle-treated iNOS remains dimeric. The dimer to monomer ratio can be visualized by differences in mobility when separated in the polyacrylamide gel matrix. Incubation of cells with SEITU (50 μ M) efficiently inhibits murine macrophage-derived iNOS activity (Fig. 4B). However, rather than reducing the amount of detectable dimer under LT SDS-PAGE conditions, SEITU increases the ratio of dimer to monomer (Fig 4A). By contrast, pretreatment with 1 μ M BBS-4 results in complete loss of detectable dimer, consistent with reports indicating that compounds in this series function as inhibitors of dimerization (Blasko et al., 2002;McMillan et al., 2000). RAW264.7 cells were treated with KLYP956 at concentrations ranging from 0.2 nM to 1 μ M. Similar to the results observed for BBS-4, KLYP956 dose dependently reduces levels of dimeric iNOS (Fig. 4A). Interestingly, unlike BBS-4, KLYP956 treatment leads to the formation of a series of one or more higher-order bands, which are likely composed of inactive multimers or oligomers of iNOS (Fig. 4A). Compounds structurally related to KLYP956 also induce the formation of these multimers (Fig. 4A and data not shown).

MOL #55434

Reduction in nitrite levels from supernatants collected from RAW264.7 cells treated with KLYP956 paralleled the reduction in dimer levels (Fig. 4B).

In order to evaluate the dimeric state of iNOS under more native conditions, we generated two epitope-tagged versions of human iNOS containing either a FLAG-tag (FLAG) or a hemagglutinin tag (HA) and cotransfected both constructs into HEK293 cells (Fig. 5A). Lysates prepared from cotransfected cells facilitated co-immunoprecipitation of the HA-tagged form using anti-FLAG antibodies (Fig. 5A). Neither HA-tagged, nor untagged native human iNOS (UT), co-immunoprecipitate with anti-FLAG antibodies in the absence of coexpressed FLAG-tagged human iNOS (Fig. 5B). This system allowed for the testing of compound effects on human iNOS protein-protein interactions under both *in vivo* and *in vitro* conditions without the need for partial denaturation. Similar to the effects seen on murine iNOS in the LT SDS-PAGE assay, SEITU treatment (50 μ M) results in somewhat greater quantities of co-immunoprecipitated HA-tagged human iNOS (Fig. 5B, upper panel). By contrast, BBS-4 has substantially reduced levels of anti-HA immunoreactivity, consistent with a reduction in dimeric human iNOS. Co-immunoprecipitated amounts of HA-tagged human iNOS are also reduced in KLYP956-treated cells, albeit to a lesser extent than that seen for BBS-4 (Fig. 5B, upper panel). In contrast, the relative levels of the iNOS-associated cofactor protein calmodulin were unaffected by any treatment tested (Fig. 5B, third panel down). Comparable levels of FLAG-iNOS were immunoprecipitated in all samples (Fig. 5B, second panel down). Enzymatic activity from cell culture supernatants treated with SEITU (50 μ M), BBS-4 (0.5 μ M) and KLYP956 (0.5 μ M) were all reduced by >95%, indicating that residual human iNOS-tagged heterodimer/multimers were inactive (Fig. 5C). To ascertain whether any of the compounds tested above could disrupt preexisting human iNOS dimers, the same cotransfection study was

MOL #55434

conducted, but with compounds added after protein expression and cell lysis. Under these conditions, vehicle-treatment of lysates results in co-immunoprecipitation of HA-tagged human iNOS, similar to that seen in the vehicle pretreatment experiment (Fig. 5B and Fig. 5D). However, none of the three compounds tested resulted in detectable changes in the level of co-immunoprecipitated HA-tagged human iNOS, even at concentrations of 50 μ M (Fig. 5D), indicating that none of these compounds can destabilize preformed iNOS dimers.

KLYP956 Destabilizes Human nNOS Dimer

Given that KLYP956 inhibits human nNOS at low micromolar concentrations, we conducted several studies to address the mechanism of inhibition of this isoform. First, we took advantage of the calcium / calmodulin dependence of nNOS to determine the ability of compounds to inhibit the enzyme in either its monomeric or dimerized state. HEK293 cells transiently transfected with human nNOS were treated with compound during the nascent phase of nNOS protein expression (within 4 hours post-transfection), or immediately prior to Ca^{2+} -ionophore activation (24 hours post-transfection), when human nNOS dimers are presumably formed. Upon activation with ionomycin, cellular human nNOS generates significant NO that is detected as nitrites using the 2,3-diaminonaphthalene reagent. Under these conditions, SEITU reduces nitrite levels with an IC_{50} of approximately 4.0 μ M and shows no change in potency or efficacy when incubated at either time point (Fig. 6A). By contrast, KLYP956 reduces nitrite levels effectively when incubated at 4 hours ($\text{IC}_{50} = 3.6 \mu\text{M}$), but shows little nitrite reduction when added immediately prior to ionophore addition ($\text{IC}_{50} > 100 \mu\text{M}$) (Fig. 6A).

The dimeric status of nNOS was assessed using LT SDS-PAGE after stably transfected human nNOS-expressing HEK293 cells were incubated with compounds. Given the long half-life

MOL #55434

reported for nNOS in cells (Kolodziejcki et al., 2004), an incubation time of 36 hours was used to ensure that the compounds were present during the synthesis of nascent nNOS protein. Lysates from treated cells were separated by LT SDS-PAGE and probed using an antibody specific for human nNOS. As seen with iNOS, SEITU increases the relative quantity of dimeric enzyme compared to vehicle-treated cells (Fig. 6B). In contrast, KLYP956 (50 μ M) reduces the level of dimeric human nNOS to an extent similar to 50 μ M BBS-4, consistent with the observed time-dependence of human nNOS inhibition seen for both compounds in figure 6A (Fig. 6B). In contrast, when compounds were incubated with nNOS expressing cells for only 1 hour, neither KLYP956 nor BBS-4 affect preexisting dimer (Fig. 6C).

Orally Administered KLYP956 Inhibits LPS-induced NO production and Attenuates Formalin-induced Nocifensive Behavior *In Vivo*

To address whether KLYP956 could inhibit iNOS activity *in vivo*, we tested the ability of the compound to reduce the production of plasma nitrates (stable metabolite of NO) in the mouse endotoxemia model. Intraperitoneal administration of lipopolysaccharide (LPS) to rodents induces a systemic inflammatory response coincident with the expression of iNOS and production of NO (Kato et al., 2005). Administration of iNOS inhibitors has been demonstrated to block the production of LPS-induced NO/nitrates (Vos et al., 1997). In agreement with *in vitro* studies, oral administration of KLYP956 reduced plasma nitrates in a dose-dependent fashion, with an ED₅₀ of approximately 10 mg/kg (Fig. 7).

Next, we investigated the ability of KLYP956 to reduce pain behaviors in a rodent model of nociceptive pain. The test involves a subcutaneous injection of dilute formalin into the plantar surface of the hind paw that causes a characteristic pattern of behavioral responses including elevation and licking of the injected paw. Two clearly demarcated phases of pain behavior,

MOL #55434

referred to as phase I (0-5 minutes post-injection) and phase II (25-45 minutes post-injection) are monitored in the model. Pain behaviors in phase II of the formalin model are thought to involve wind-up of spinal neurons in a process referred to as central sensitization (Dubuisson and Dennis, 1977). Efficacy of KLYP956 in attenuating nocifensive behavior elicited by intraplantar injection of formalin was assessed both after intraperitoneal and oral routes of administration. Intraperitoneal injection of KLYP956 (30 mg/kg) given 1 hour before intraplantar injection of formalin attenuated both the phase I and phase II of the pain response with a more robust effect on phase II (86% reduction, $p < 0.01$ versus vehicle), indicating that this compound affects central sensitization (Fig. 8A). Oral administration of KLYP956 (30 and 100 mg/kg) given one hour in advance of formalin injection led to dose-related decrements in both phase I and Phase II nocifensive behaviors (Figure 8B). The attenuation of formalin-induced nocifensive behavior by KLYP956 was similar to the previously described iNOS inhibitor AR-C102222 (AR) and was not sensitive to the opiate antagonist, naloxone (Fig. 8A and data not shown).

Discussion

A plethora of iNOS inhibitors have been described, with the majority representing classical substrate competitive inhibitors that share structural similarity to the amino acid arginine (Vallance and Leiper, 2002). Given the potential issues associated with this class of molecules and the paucity of viable clinical candidates, efforts to identify alternative mechanisms of enzyme inhibition have been undertaken by several groups (Paige and Jaffrey, 2007). The identification of imidazole-containing anti-fungal agents that interfere with iNOS dimerization has prompted the discovery of several classes of related small molecule dimerization inhibitors

MOL #55434

(DI) (Sennequier et al., 1999). Much like the anti-fungal inhibitors, the inhibitory activity of these compounds is completely dependent upon an imidazole group, which coordinates the heme iron within the catalytic domain of the enzyme (McMillan et al., 2000). While these agents may overcome some of the pitfalls associated with arginine mimetics, we hypothesized that alternatives to an imidazole-dependent mechanism of dimer destabilization may prove beneficial in minimizing potential liabilities such as interaction with other heme-containing enzymes, including cytochrome P450s (Albengres et al., 1998;Zhang et al., 2002).

The quinolinone, KLYP956, arose from an ultra high-throughput screening and medicinal chemistry effort that was designed to identify iNOS inhibitors with novel mechanisms of action, such as dimer destabilization. The sensitivity and low cost of the homogeneous primary assay used in the screen enabled profiling of a larger compound collection than has heretofore been reported for other iNOS screening campaigns. A previous report proposed that activated murine macrophage RAW264.7 cells could be used in a primary screen to identify inhibitors of human iNOS, based on the considerable amino acid and structural conservation between the active sites of these enzymes (Naureckiene et al., 2007). However, the precursor to KLYP956 identified in the screening campaign was virtually inactive against murine iNOS (KS, CH unpublished observations). KLYP956 itself exhibits a 14-fold preference for human iNOS versus murine iNOS. Therefore our studies clearly demonstrate the existence of species selective iNOS inhibitors. Perhaps even more surprising are the apparent differences in KLYP956 potency against iNOS and nNOS between the two species. There exists a 260-fold difference in potency of KLYP956 between human iNOS and human nNOS. In contrast, KLYP956 inhibits murine iNOS and nNOS with nearly identical potencies. Recent structural studies may provide insight

MOL #55434

into the molecular basis of these effects. Examination of the binding mode of a series of quinazoline and aminopyridine inhibitors (Garcin et al., 2008) revealed that flexibility in a triad of sequence divergent second- and third-shell residues can regulate conformational switching in the absolutely conserved residues lining the active site of iNOS, particularly that of a highly conserved glutamine residue (Gln257/263 in murine/human iNOS). Molecular modeling of the binding mode of KLYP956 suggests that it could form nonpolar contacts with Gln257/263. If this were to be the case, KLYP956 inhibitory potency might be determined by residues significantly distal to the active site. These sequence differences, combined with evidence that eNOS forms a more stable dimer than the other two isoforms (Panda et al., 2002), may also explain the considerable selectivity of KLYP956 against both human and murine eNOS. Further studies will be required to determine the features that underlie the isoform and unexpected species selectivity of KLYP956.

Mechanistic analysis from cell-based and biochemical inhibition studies suggest that, unlike substrate competitive inhibitors like SEITU, KLYP956 cannot inhibit NOS activity of stable intact dimers. Data suggest that KLYP956 may bind iNOS and nNOS in a monomeric or loose dimeric state and interfere with the formation of a stable, enzymatically active dimer. The identification of a quinolinone-based NOS dimerization inhibitor provides evidence that direct imidazole-based coordination of the heme iron is not required for iNOS and nNOS dimer destabilization. Several lines of evidence suggest that chemical differences between BBS-4 and KLYP956 lead to differences in the inhibitory mechanism of the two compounds. First, heme spectral studies indicate an interaction for both compounds in the vicinity of the active site. However, binding of imidazole is mediated through direct coordination with the heme iron,

MOL #55434

leading to a single Soret band with an absorbance maximum at 429 nm (Sennequier and Stuehr, 1996). This contrasts sharply with the spectral shift induced by KLYP956, where a single broad maximum at 396 nm is generated (Fig. 3). The shift to 396 nm is more akin to that induced by the addition of arginine and tetrahydrobiopterin to iNOS monomers, although in this latter case, dimerization is actually augmented (Sennequier et al., 1999). The binding mode may be similar to that of previously described coumarin-based substrate-competitive inhibitors (Jackson et al., 2005). A second difference in mechanism of dimer destabilization can be inferred from LT SDS-PAGE data from RAW264.7 cells treated with compounds. In these studies, treatment with KLYP956 and related molecules induces higher-order species that are detected with iNOS specific antibodies (Fig. 4A and data not shown). The formation of inactive multimeric iNOS may help explain the less pronounced reduction in HA-tagged human iNOS protein that is detected in KLYP956-treated versus BBS-4-treated coimmunoprecipitation experiments (Fig. 5B). Calmodulin is an essential protein cofactor known to form a tight interaction with iNOS even at low levels of intracellular calcium (Vallance and Leiper, 2002). Notably, the association of iNOS with calmodulin appears to be unaffected by KLYP956, based on coimmunoprecipitation studies, suggesting that disruption of this protein-protein interaction does not contribute to the compound's mechanism of action (Fig 5B). In summary, the overall similarity between the NOS inhibitory profiles of BBS-4 and KLYP956 suggest that the latter acts via destabilization of iNOS and nNOS dimers, although details of the modes of action may differ between the two compounds. A peptide-based compound lacking an imidazole has been described to have iNOS dimer destabilizing properties, providing further evidence that an imidazole is not essential for this mechanism of inhibition (Chida et al., 2005).

MOL #55434

In addition, several endogenous proteins have been described that modulate the quaternary structure of iNOS and nNOS (Kone et al., 2003). The cumulative data suggest that both NOS isoforms may have evolved intrinsic capacities to modulate activity by regulating the extent and stability of homodimerization. This is further supported by earlier site-directed mutagenesis studies demonstrating that single amino acid changes in the dimerization interface of iNOS abrogates dimer formation (Ghosh et al., 1999). Given the multifaceted role of arginine in the body, mechanisms may have evolved to regulate this enzyme class independently of substrate concentration. Our work, along with that of several other groups, indicates that this regulation of NOS quaternary structure can be exploited to generate novel therapeutics. Toward this end, we have identified KLYP956, which inhibits iNOS and nNOS dimerization and enzymatic activity both in biochemical assays and in cells. Even more importantly, administration of KLYP956 in animals results in the inhibition of iNOS activity and attenuation of nociceptive behaviors, indicating that the mechanism of action is functional *in vivo*. In conclusion, the potency, selectivity and mechanism of inhibition of KLYP956 provide the potential that such an agent could become a viable pharmaceutical alternative to existing NOS inhibitors.

Acknowledgements

We thank Thomas Lee for assistance with potency/selectivity assays and Dennis Stuehr for helpful discussions and review of the manuscript.

References

Albengres E, Le L H and Tillement J P (1998) Systemic Antifungal Agents. Drug Interactions of Clinical Significance. *Drug Saf* **18**:83-97.

MOL #55434

Blasko E, Glaser C B, Devlin J J, Xia W, Feldman R I, Polokoff M A, Phillips G B, Whitlow M, Auld D S, McMillan K, Ghosh S, Stuehr D J and Parkinson J F (2002) Mechanistic Studies With Potent and Selective Inducible Nitric-Oxide Synthase Dimerization Inhibitors. *J Biol Chem* **277**:295-302.

Chida N, Hirasawa Y, Ohkawa T, Ishii Y, Sudo Y, Tamura K and Mutoh S (2005) Pharmacological Profile of FR260330, a Novel Orally Active Inducible Nitric Oxide Synthase Inhibitor. *Eur J Pharmacol* **509**:71-76.

Davey DD, Adler M, Arnaiz D, Eagen K, Erickson S, Guilford W, Kenrick M, Morrissey M M, Ohlmeyer M, Pan G, Paradkar V M, Parkinson J, Polokoff M, Saionz K, Santos C, Subramanyam B, Vergona R, Wei R G, Whitlow M, Ye B, Zhao Z S, Devlin J J and Phillips G (2007) Design, Synthesis, and Activity of 2-Imidazol-1-Ylpyrimidine Derived Inducible Nitric Oxide Synthase Dimerization Inhibitors. *J Med Chem* **50**:1146-1157.

Dubuisson D and Dennis S G (1977) The Formalin Test: a Quantitative Study of the Analgesic Effects of Morphine, Meperidine, and Brain Stem Stimulation in Rats and Cats. *Pain* **4**:161-174.

Edwards RM, Stack E J and Trizna W (1998) Interaction of L-Arginine Analogs With L-Arginine Uptake in Rat Renal Brush Border Membrane Vesicles. *J Pharmacol Exp Ther* **285**:1019-1022.

Feldman PL, Griffith O W, Hong H and Stuehr D J (1993) Irreversible Inactivation of Macrophage and Brain Nitric Oxide Synthase by L-NG-Methylarginine Requires NADPH-Dependent Hydroxylation. *J Med Chem* **36**:491-496.

Garcin ED, Arvai A S, Rosenfeld R J, Kroeger M D, Crane B R, Andersson G, Andrews G, Hamley P J, Mallinder P R, Nicholls D J, St-Gallay S A, Tinker A C, Gensmantel N P, Mete A, Cheshire D R, Connolly S, Stuehr D J, Aberg A, Wallace A V, Tainer J A and Getzoff E D (2008) Anchored Plasticity Opens Doors for Selective Inhibitor Design in Nitric Oxide Synthase. *Nat Chem Biol* **4**:700-707.

Ghosh S, Wolan D, Adak S, Crane B R, Kwon N S, Tainer J A, Getzoff E D and Stuehr D J (1999) Mutational Analysis of the Tetrahydrobiopterin-Binding Site in Inducible Nitric-Oxide Synthase. *J Biol Chem* **274**:24100-24112.

Jackson SA, Sahni S, Lee L, Luo Y, Nieduzak T R, Liang G, Chiang Y, Collar N, Fink D, He W, Laoui A, Merrill J, Boffey R, Crackett P, Rees B, Wong M, Guilloteau J P, Mathieu M and Rebello S S (2005) Design, Synthesis and Characterization of a Novel Class of Coumarin-Based Inhibitors of Inducible Nitric Oxide Synthase. *Bioorg Med Chem* **13**:2723-2739.

Kato H, Negoro M and Wakabayashi I (2005) Effects of Acute Ethanol Administration on LPS-Induced Expression of Cyclooxygenase-2 and Inducible Nitric Oxide Synthase in Rat Alveolar Macrophages. *Alcohol Clin Exp Res* **29**:285S-293S.

Kolodziejwski PJ, Koo J S and Eissa N T (2004) Regulation of Inducible Nitric Oxide Synthase by Rapid Cellular Turnover and Cotranslational Down-Regulation by Dimerization Inhibitors. *Proc Natl Acad Sci U S A* **101**:18141-18146.

MOL #55434

Kone BC, Kuncewicz T, Zhang W and Yu Z Y (2003) Protein Interactions With Nitric Oxide Synthases: Controlling the Right Time, the Right Place, and the Right Amount of Nitric Oxide. *Am J Physiol Renal Physiol* **285**:F178-F190.

Labuda CJ, Koblisch M, Tuthill P, Dolle R E and Little P J (2005) Antinociceptive Activity of the Selective INOS Inhibitor AR-C102222 in Rodent Models of Inflammatory, Neuropathic and Post-Operative Pain. *Eur J Pain* 10:505-512.

Li D, Hayden E Y, Panda K, Stuehr D J, Deng H, Rousseau D L and Yeh S R (2006) Regulation of the Monomer-Dimer Equilibrium in Inducible Nitric-Oxide Synthase by Nitric Oxide. *J Biol Chem* **281**:8197-8204.

McMillan K, Adler M, Auld D S, Baldwin J J, Blasko E, Browne L J, Chelsky D, Davey D, Dolle R E, Eagen K A, Erickson S, Feldman R I, Glaser C B, Mallari C, Morrissey M M, Ohlmeyer M H, Pan G, Parkinson J F, Phillips G B, Polokoff M A, Sigal N H, Vergona R, Whitlow M, Young T A and Devlin J J (2000) Allosteric Inhibitors of Inducible Nitric Oxide Synthase Dimerization Discovered Via Combinatorial Chemistry. *Proc Natl Acad Sci U S A* **97**:1506-1511.

McMillan K and Masters B S (1993) Optical Difference Spectrophotometry As a Probe of Rat Brain Nitric Oxide Synthase Heme-Substrate Interaction. *Biochemistry* **32**:9875-9880.

Naureckiene S, Edris W, Ajit S K, Katz A H, Sreekumar K, Rogers K E, Kennedy J D and Jones P G (2007) Use of a Murine Cell Line for Identification of Human Nitric Oxide Synthase Inhibitors. *J Pharmacol Toxicol Methods* **55**:303-313.

Ohtsuka M, Konno F, Honda H, Oikawa T, Ishikawa M, Iwase N, Isomae K, Ishii F, Hemmi H and Sato S (2002) PPA250 [3-(2,4-Difluorophenyl)-6-[2-[4-(1H-Imidazol-1-ylmethyl)Phenoxy]Ethoxy]-2-Phenylpyridine], a Novel Orally Effective Inhibitor of the Dimerization of Inducible Nitric-Oxide Synthase, Exhibits an Anti-Inflammatory Effect in Animal Models of Chronic Arthritis. *J Pharmacol Exp Ther* **303**:52-57.

Olken NM, Osawa Y and Marletta M A (1994) Characterization of the Inactivation of Nitric Oxide Synthase by NG-Methyl-L-Arginine: Evidence for Heme Loss. *Biochemistry* **33**:14784-14791.

Paige JS and Jaffrey S R (2007) Pharmacologic Manipulation of Nitric Oxide Signaling: Targeting NOS Dimerization and Protein-Protein Interactions. *Curr Top Med Chem* **7**:97-114.

Panda K, Rosenfeld R J, Ghosh S, Meade A L, Getzoff E D and Stuehr D J (2002) Distinct Dimer Interaction and Regulation in Nitric-Oxide Synthase Types I, II, and III. *J Biol Chem* **277**:31020-31030.

Robertson CA, Green B G, Niedzwiecki L, Harrison R K and Grant S K (1993) Effect of Nitric Oxide Synthase Substrate Analog Inhibitors on Rat Liver Arginase. *Biochem Biophys Res Commun* **197**:523-528.

MOL #55434

Sennequier N and Stuehr D J (1996) Analysis of Substrate-Induced Electronic, Catalytic, and Structural Changes in Inducible NO Synthase. *Biochemistry* **35**:5883-5892.

Sennequier N, Wolan D and Stuehr D J (1999) Antifungal Imidazoles Block Assembly of Inducible NO Synthase into an Active Dimer. *J Biol Chem* **274**:930-938.

Siddhanta U, Presta A, Fan B, Wolan D, Rousseau D L and Stuehr D J (1998) Domain Swapping in Inducible Nitric-Oxide Synthase. Electron Transfer Occurs Between Flavin and Heme Groups Located on Adjacent Subunits in the Dimer. *J Biol Chem* **273**:18950-18958.

Sohn MJ, Hur G M, Byun H S and Kim W G (2008) Cyclo(Dehydrohistidyl-L-Tryptophyl) Inhibits Nitric Oxide Production by Preventing the Dimerization of Inducible Nitric Oxide Synthase. *Biochem Pharmacol* **75**:923-930.

Vallance P and Leiper J (2002) Blocking NO Synthesis: How, Where and Why? *Nat Rev Drug Discov* **1**:939-950.

Vos TA, Gouw A S, Klok P A, Havinga R, Van G H, Huitema S, Roelofsen H, Kuipers F, Jansen P L and Moshage H (1997) Differential Effects of Nitric Oxide Synthase Inhibitors on Endotoxin-Induced Liver Damage in Rats. *Gastroenterology* **113**:1323-1333.

Wang W and Malcolm B A (1999) Two-Stage PCR Protocol Allowing Introduction of Multiple Mutations, Deletions and Insertions Using QuikChange Site-Directed Mutagenesis. *Biotechniques* **26**:680-682.

Zhang W, Ramamoorthy Y, Kilicarslan T, Nolte H, Tyndale R F and Sellers E M (2002) Inhibition of Cytochromes P450 by Antifungal Imidazole Derivatives. *Drug Metab Dispos* **30**:314-318.

MOL #55434

Figure Legends

Fig. 1. Chemical Structure of KLYP956 and other known iNOS inhibitors

- A. KLYP956 is a novel N-(3-chlorophenyl)-N-((8-fluoro-2-oxo-1,2-dihydroquinolin-4-yl)methyl)-4-methylthiazole-5-carboxamide inhibitor of iNOS, a precursor of which was identified in a cell-based ultra high-throughput screen
- B. SEITU (S-ethyl-isothiourea) is a non-selective substrate-competitive inhibitor of NOS that is isosteric with L-arginine; BBS-4 is an N-substituted imidazole-containing inhibitor of iNOS dimerization

Fig. 2. KLYP956 inhibits iNOS in cells but not in reconstituted biochemical assays

- A. Cell-based iNOS inhibition assay; recombinant iNOS (human iNOS or murine iNOS) was transiently transfected into HEK293 cells and NO production was measured indirectly by measuring nitrite levels using 2,3-diaminonaphthalene reagent (DAN). Data are shown as dose-response curves of iNOS inhibition \pm SD of KLYP956 against human (●) and murine (■) iNOS, respectively.
- B. Biochemical inhibition of human iNOS; compounds (SEITU, ▲; BBS-4, ●; KLYP956, ■) were incubated for 20 minutes with protein extracts derived from HEK293 cells transfected with human iNOS followed by measuring conversion of radioactive arginine to citrulline. Data are shown as dose-response curves of iNOS inhibition, mean \pm SD.
- C. Biochemical inhibition of human nNOS; compounds (SEITU, ▼; BBS-4, ●; KLYP956, ■) were incubated for 20 minutes with protein extracts derived from HEK293 cells

MOL #55434

transfected with human nNOS followed by measuring conversion of radioactive arginine to citrulline. Data are shown as dose-response curves of nNOS inhibition, mean \pm SD.

Fig. 3. KLYP956 perturbs purified iNOS_{oxy} domain heme absorbance spectrum *in vitro*

Urea-dialyzed human iNOS_{oxy} (residues 74-504) displays a characteristic twin Soret absorbance spectrum with peaks at 378 nm and 460 nm. KLYP956 dose-dependently induces a spin state transition of the heme iron to generate an absorbance maxima of 396 nm. Each trace represents a distinct concentration of KLYP956 as indicated on the graph: 0 μ M (—), 1 μ M (---), 3 μ M (- - -), and 10 μ M (—). Arrows indicate the increase and decrease in absorbance at 396 nm and 460 nm, respectively. Inset displays a reciprocal difference plot between changes in absorbance at 396 nm and 460 nm versus KLYP956 concentration. Line represents best fit using least squares method ($r^2 = 0.9998$).

Fig. 4. KLYP956 destabilizes murine iNOS dimer in cells

A. LPS/IFN- γ induced RAW264.7 cells treated with indicated compounds for 18 hours were lysed and proteins were separated by low temperature SDS-PAGE and transferred to nitrocellulose and immunoblotted against iNOS. Compounds were tested at the following concentrations SEITU (50 μ M); BBS-4 (1 μ M), KLYP956 was tested in dose-response: 1000 nM, 250 nM, 62.5 nM, 16 nM, 4 nM, 1nM, 0.2 nM. Proteins cross-reacting with anti-iNOS antibodies corresponding to different forms of iNOS are indicated (monomer, dimer, multimer).

MOL #55434

- B. Cell culture supernatant obtained from RAW264.7 cells used in Figure 4A was tested for nitrite levels using 2,3-diaminonaphthalene (DAN) assay. Vehicle (■, DMSO) and SEITU (▲, 50 μ M) is used to define 0% and 100% inhibition, respectively. KLYP956 (●) reduces iNOS activity in a concentration-dependent fashion. Data are shown as percent inhibition of iNOS activity and are representative of three independent experiments.

Fig. 5. KLYP956 destabilizes human iNOS dimer in cells

- A. Schematic representing coimmunoprecipitation / Western blotting experimental procedure used to investigate quaternary structure of recombinant human iNOS. In the absence of dimerization inhibitors (DI), iNOS dimerization is permitted, allowing for the formation of FLAG-HA heterodimers (as well as FLAG-FLAG and HA-HA homodimers). Anti-FLAG immunoprecipitation (IP) facilitates isolation of complexes containing FLAG-tagged proteins. Anti-HA antibodies detect immunoprecipitated proteins containing the HA sequence. However, in the presence of DI, dimerization of iNOS is blocked resulting in the absence of coimmunoprecipitated HA-tagged iNOS.
- B. HA-tagged (HA) and FLAG-tagged (FLAG) human iNOS expression constructs were cotransfected into HEK293 cells treated with compounds at the following concentrations (SEITU, 50 μ M; BBS-4, 0.5 μ M; KLYP956, 0.5 μ M). Cells were lysed after 18 hours of coincubation with compound. FLAG-tagged proteins from lysates were immunoprecipitated with anti-FLAG antibodies and proteins were separated by SDS-PAGE, transferred to nitrocellulose and probed with anti-HA antibody (upper panel), anti-FLAG antibody (second panel down), or anti-calmodulin (CaM) antibody (third panel down). Lysate input was examined to ensure equivalent expression of HA-tagged

MOL #55434

iNOS (lower panel). Singly-transfected untagged native human iNOS (UT) and HA-tagged human iNOS demonstrates specificity of anti-HA western blotting and anti-FLAG immunoprecipitating antibodies, respectively.

C. iNOS enzymatic activity from compound-treated cells: cell culture supernatant from compound-treated cells in Figure 5B were tested for nitrite levels (DAN assay).

Comparable levels of iNOS activity are present in untagged (UT), HA-tagged (HA), or cotransfected FLAG and HA samples. All three inhibitors reduce enzyme activity by >95%. Data are shown as Mean + SEM, *** $p < 0.0001$, t-test.

D. KLYP956 does not disrupt preexisting iNOS dimers *in vitro*. HA-tagged (HA) and FLAG-tagged (FLAG) human iNOS expression constructs were cotransfected into HEK293 cells as described above, but in the absence of compounds, and lysates were prepared. Compounds were then incubated with lysates for 1 hour prior to immunoprecipitation. Lysates were incubated with anti-FLAG antibodies for an additional hour and immunoprecipitated proteins were separated by SDS-PAGE and transferred to nitrocellulose and probed with anti-HA antibody (upper panel) or anti-FLAG antibody (lower panel). Input is equivalent to 1/6th of the material used for immunoprecipitated samples.

Fig. 6. KLYP956 destabilizes human nNOS dimer.

A. Transiently transfected HEK293 cells expressing recombinant human nNOS were treated with compound either 4 hrs or 24 hrs post-transfection. Cells were activated with calcium ionophore for 18 hrs and nitrites (nNOS activity) were measured using DAN assay. Data are represented in dose-response as percent enzyme inhibition mean

MOL #55434

± SD for compounds as indicated: SEITU, 4 hrs (●); SEITU, 24 hrs (■); KLYP956, 4 hrs (▲); KLYP956, 24 hrs (▼).

B. Immunoblot of human nNOS LT-SDS-PAGE with compound pretreatment.

HEK293 cells stably transfected with human nNOS were treated with compound indicated (50 μM) for 36 hrs and lysates were prepared. Proteins from lysates were separated by low temperature SDS-PAGE and transferred to nitrocellulose and probed with an anti-nNOS antibody. Dimeric (dimer) and monomeric (monomer) nNOS are indicated with arrows. Untransfected wild-type HEK293 cells (UT) do not express proteins that cross-react with anti-nNOS antibodies under these conditions.

C. Immunoblot of human nNOS LT-SDS-PAGE with pre-formed dimer.

HEK293 cells stably transfected with human nNOS were treated with compound indicated (50 μM) for 1 hr and lysates were prepared. Proteins from lysates were separated by low temperature SDS-PAGE and transferred to nitrocellulose and probed with an anti-nNOS antibody as described above.

Fig. 7. KLYP956 inhibits LPS-induced nitrite production *in vivo* (oral administration).

Plasma collected from compound-treated Balb /C mice 6 hrs post LPS injection was measured for nitrite/nitrate concentrations (indirect measure of iNOS activity). KLYP956 was administered orally at the doses indicated (mg/kg) immediately prior to LPS challenge.

MOL #55434

Calculated ED₅₀ = 10 mg/kg. Data are represented as mean + SEM; *p<0.05, ***p<0.001 as compared to LPS alone, Dunnett's test.

Fig. 8. KLYP956 inhibits nocifensive behaviors in the mouse formalin model

KLYP956 (30 mg/kg) or AR-C102222 (AR, 30 mg/kg) (Labuda et al., 2005) were delivered via intraperitoneal injection (**A**) or via oral gavage for KLYP956 at 30 and 100 mg/kg (**B**) 1 hour prior to formalin injection into the hind paw of male Balb /C mice. Duration of pain behaviors (flinching, biting, licking) were quantified for both phase I (0-5 minutes) and phase II (25-40 minutes) and results are shown as mean + SEM (*p < 0.05, **p < 0.01, ***p < 0.001 as compared to vehicle (Veh)).

MOL #55434

Table 1.
KLYP956 isoform and species selectivity profile

Species	iNOS (μM)	nNOS (μM)	eNOS (μM)	i/n Selectivity	i/e Selectivity
Human	0.01 +/- 0.01	2.6 +/- 1.0	19 +/- 6.5	260-fold	1900-fold
Murine	0.14 +/- 0.12	0.15 +/- 0.05	12.0 +/- 4.8	non-selective	86-fold

Values in second, third and fourth column represent IC_{50} +/- SD for NOS inhibition. Calculations are averages of at least three experiments.

MOL #55434

Table 2.
KLYP956 is non-arginine competitive in cells

Arginine [μM]	10	1000	
Compound	IC_{50} (μM)	IC_{50} (μM)	Fold Shift
KLYP956	0.005 +/- 0.001	0.010 +/- 0.004	2
BBS-4	0.005 +/- 0.002	0.007 +/- 0.001	<2
SEITU	2.2 +/- 1.0	29.1 +/- 8.3	15
1400W	3.9 +/- 2.2	34.9 +/- 16.3	9

Values in second and third column represent IC_{50} +/- SD for iNOS inhibition. Calculations are averages of three experiments.

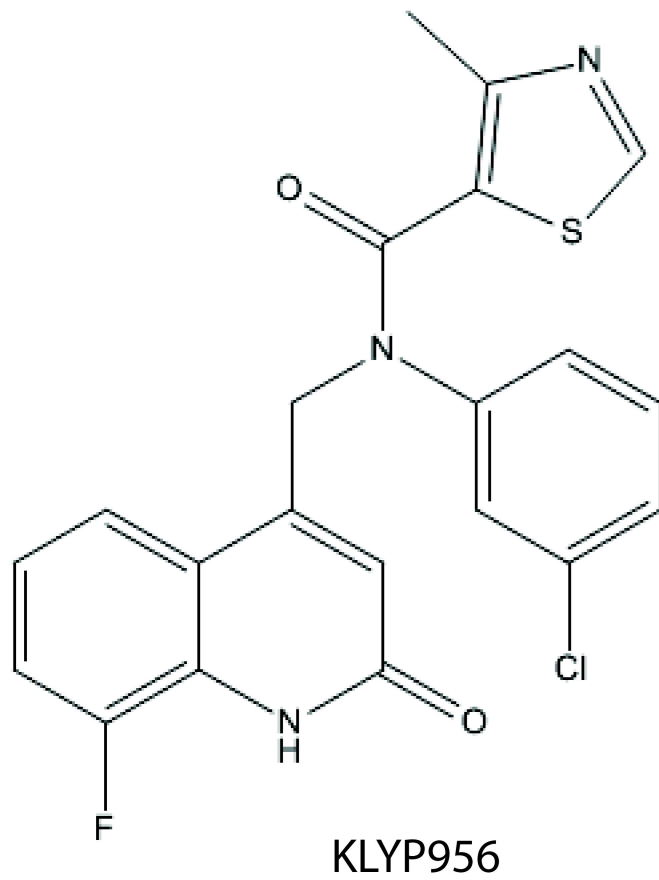
MOL #55434

Table 3.
KLYP956 is non-biopterin competitive in cells

Sepiapterin [μM]	0	1	10
Compound	IC_{50} (μM)	IC_{50} (μM)	IC_{50} (μM)
KLYP956	0.002 +/- 0.001	0.002 +/- 0.001	0.002 +/- 0.001
BBS-4	0.002 +/- 0.001	0.003 +/- 0.001	0.003 +/- 0.001
SEITU	1.8 +/- 0.2	1.5 +/- 0.8	1.5 +/- 0.2

Values represent IC_{50} +/- SD for iNOS inhibition. Calculations are averages of three experiments.

A



B

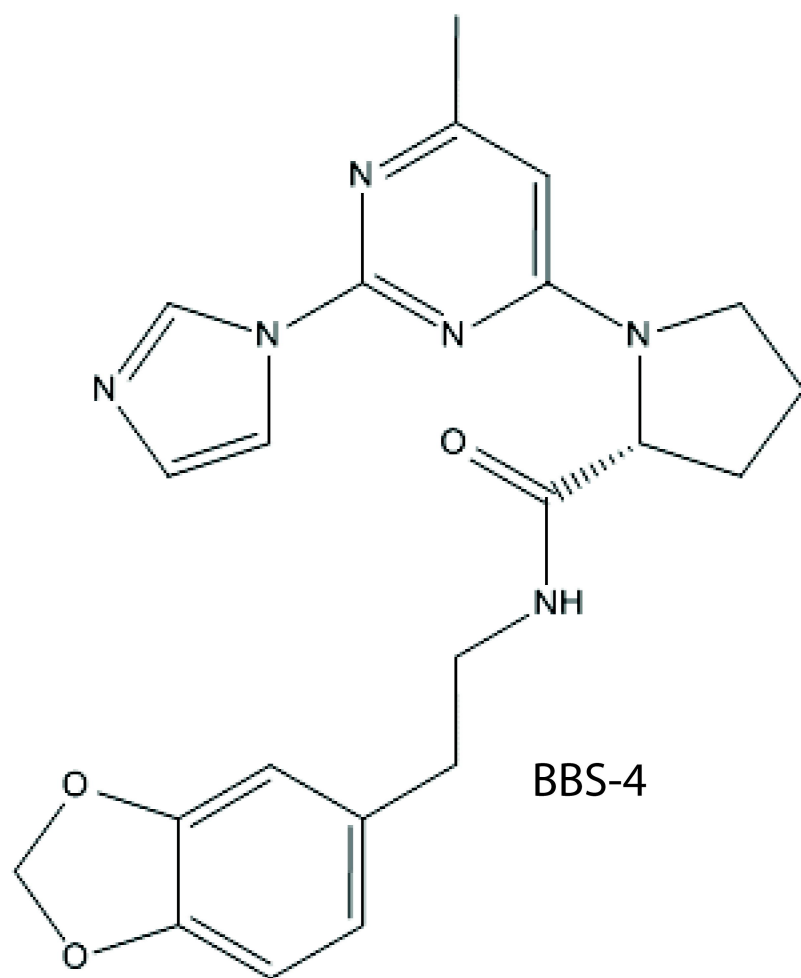
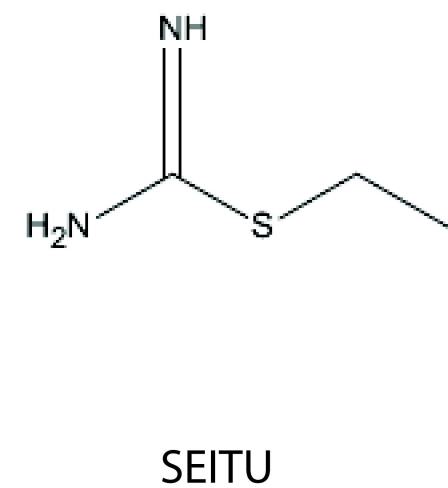
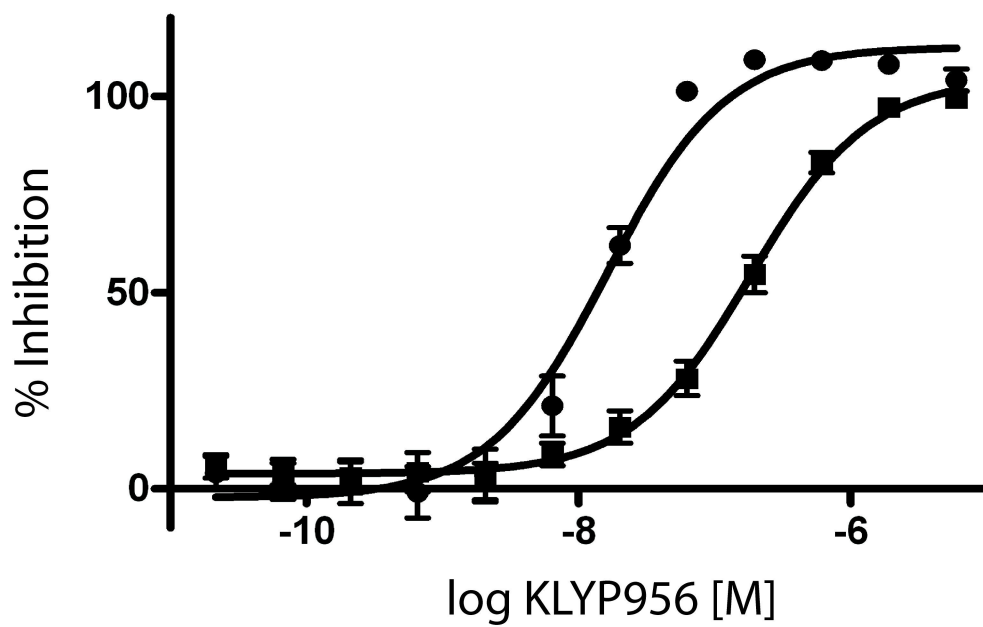
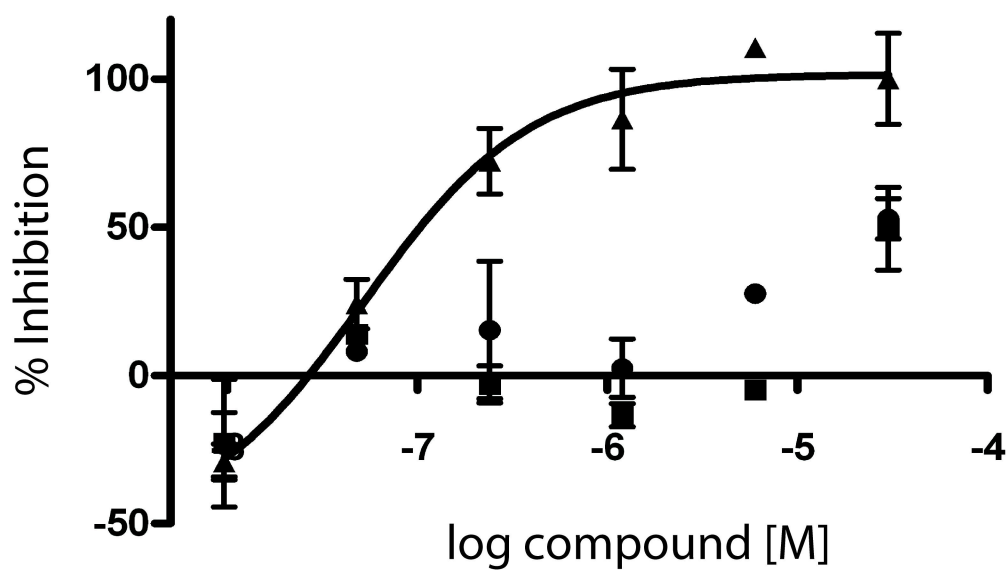


Figure 1

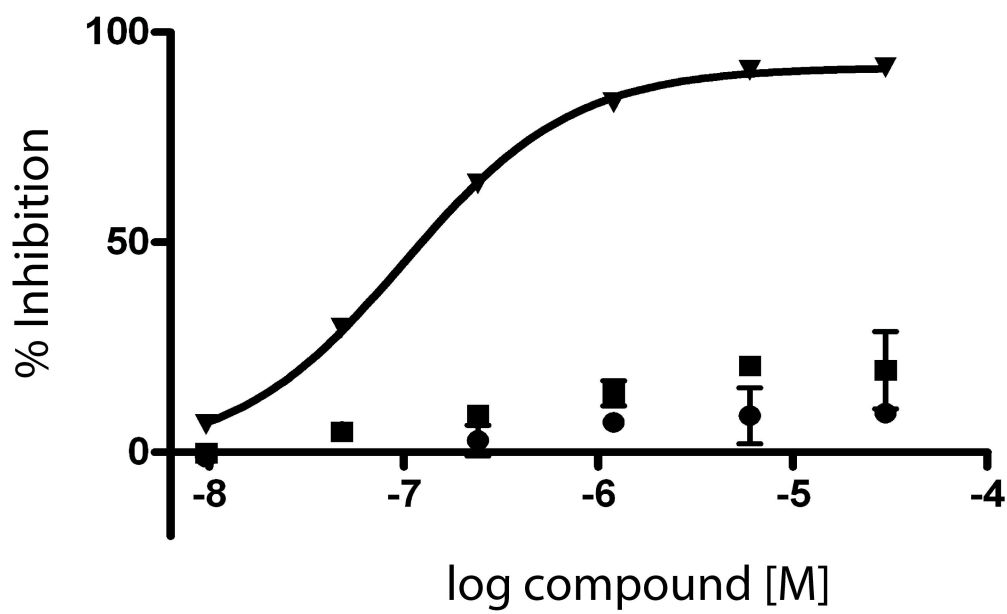
A

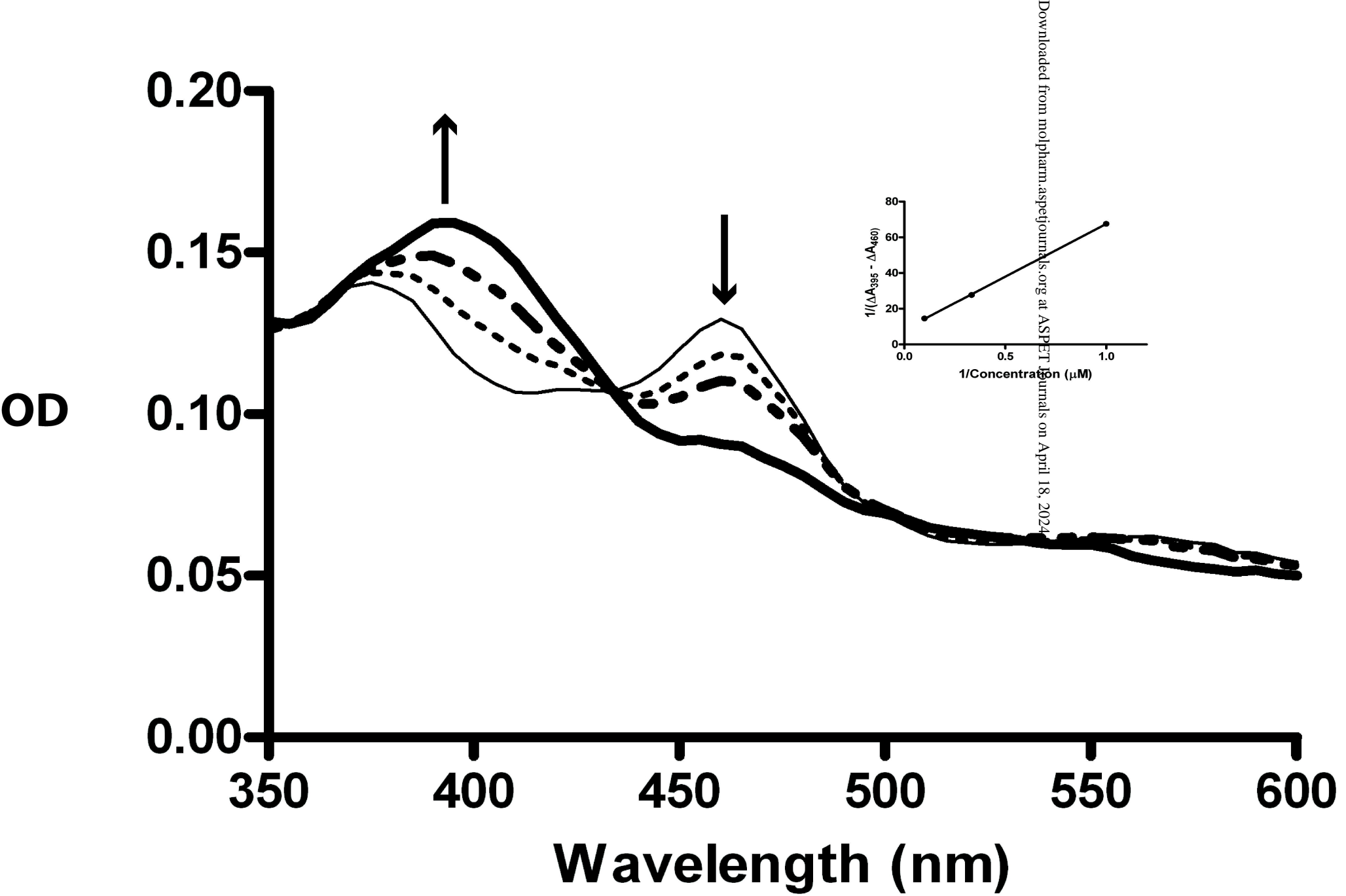


B



C

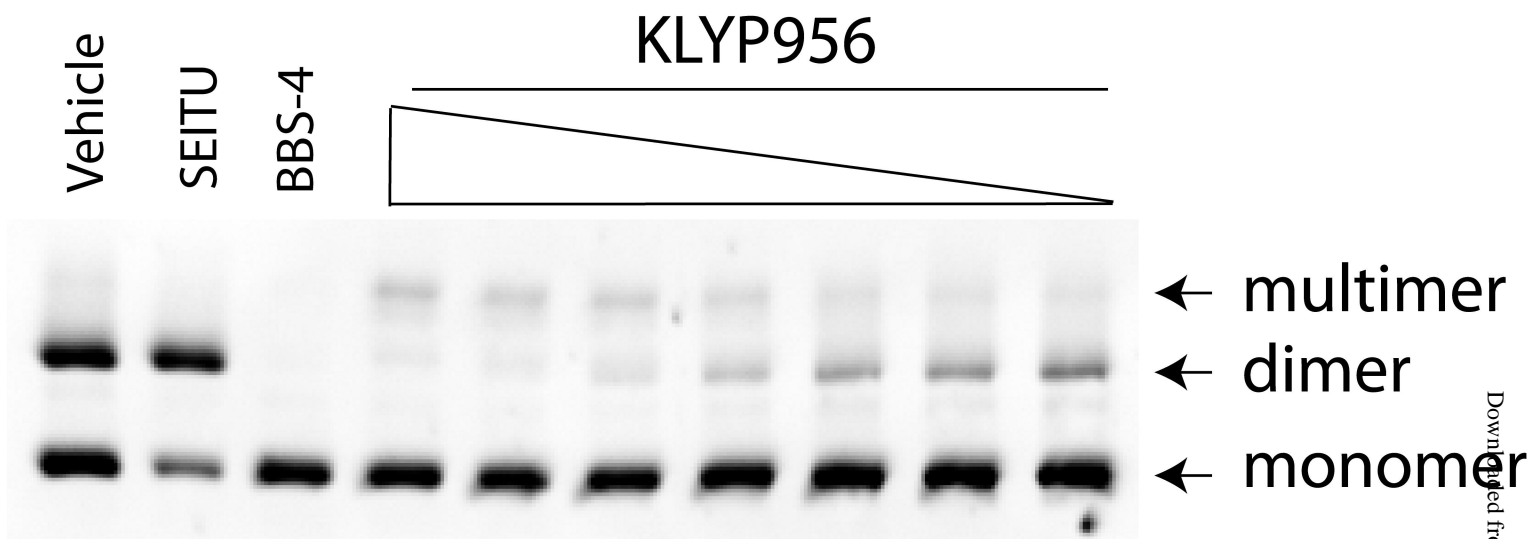




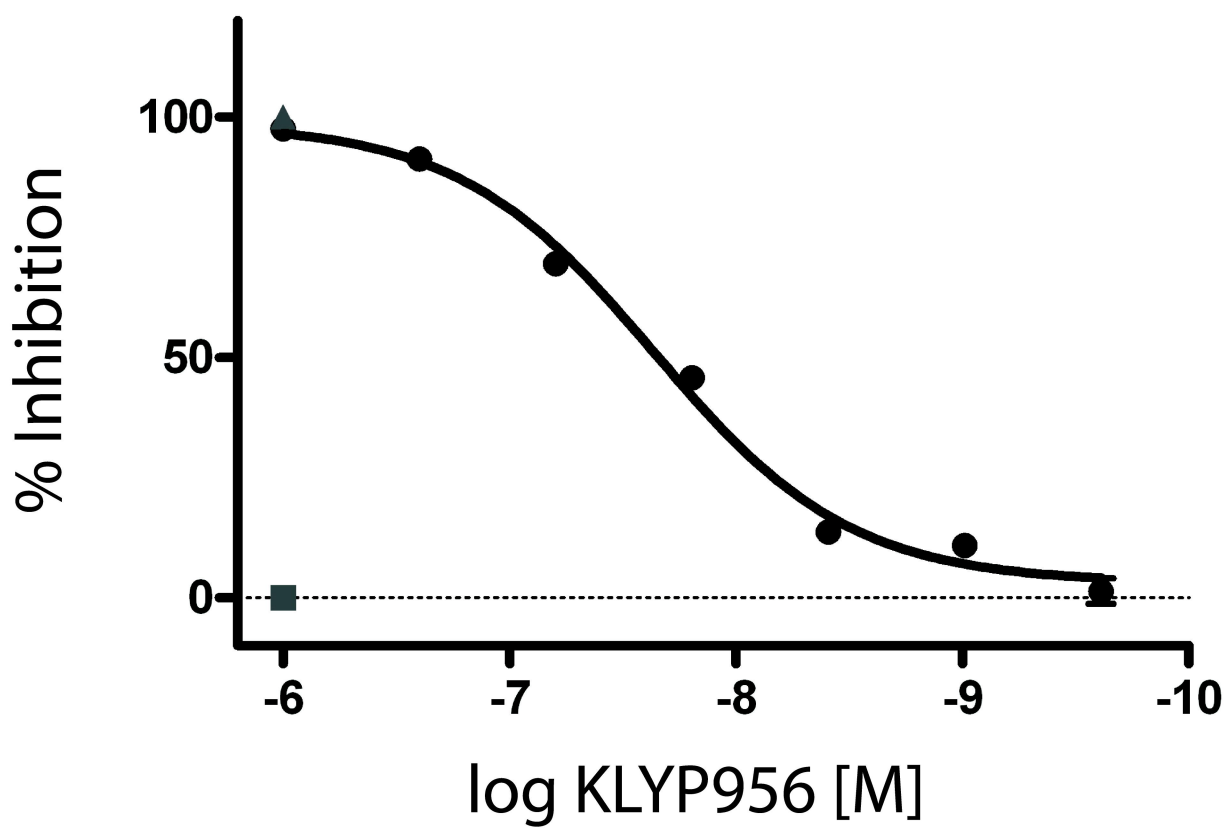
Downloaded from molpharm.aspetjournals.org at ASPET Journals on April 18, 2024

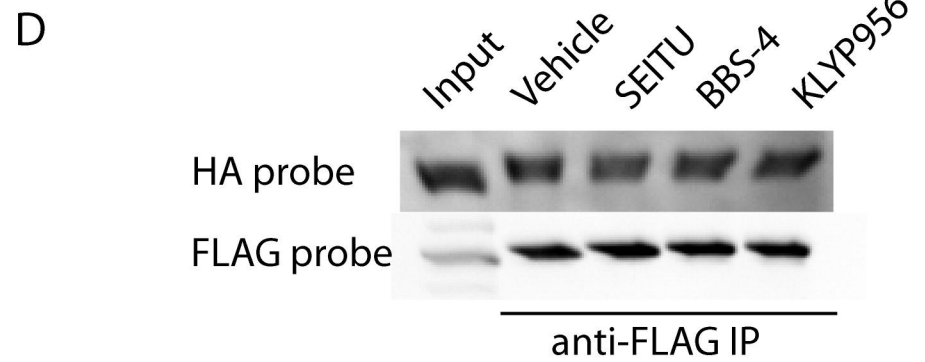
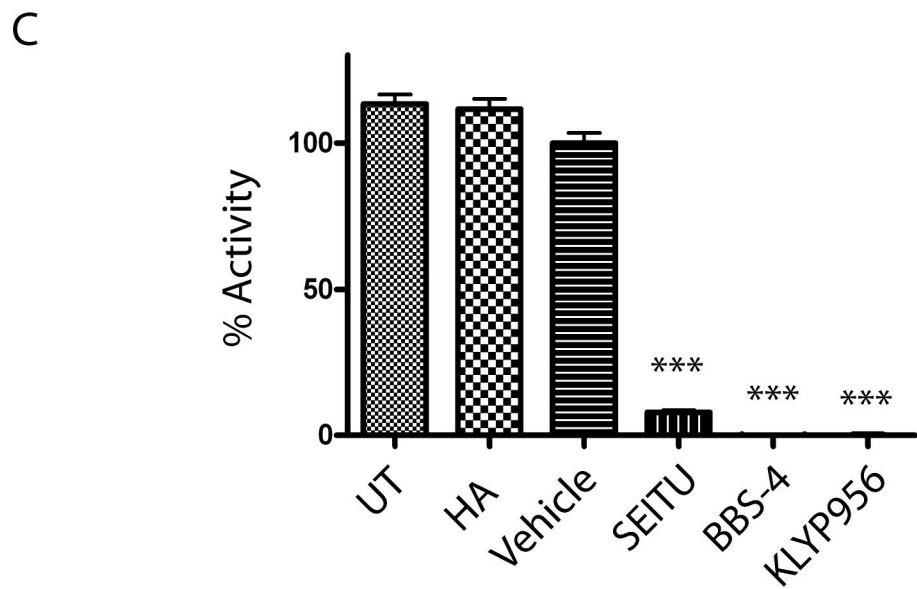
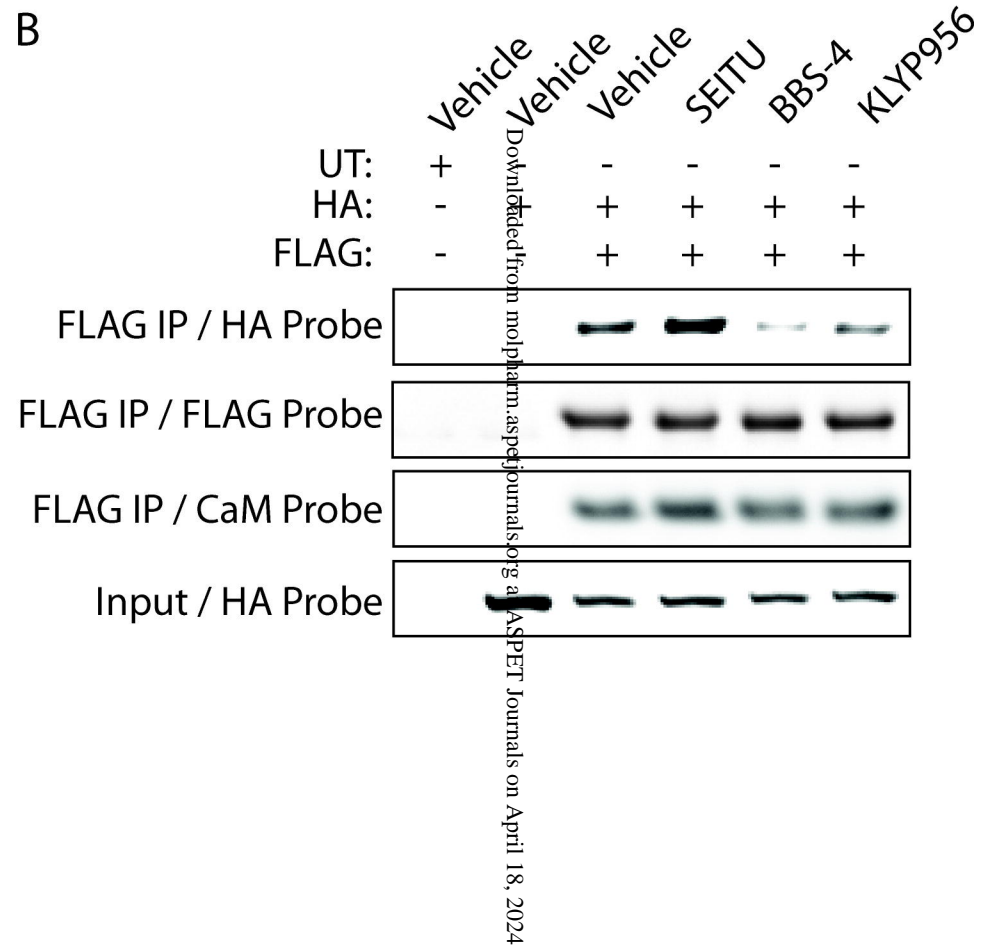
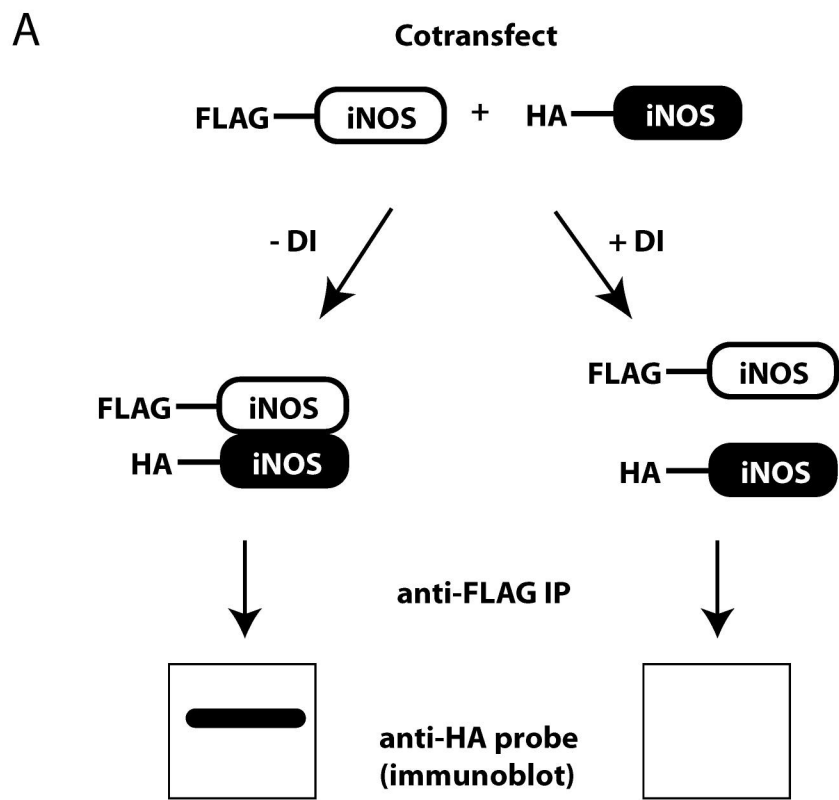
Figure 3

A

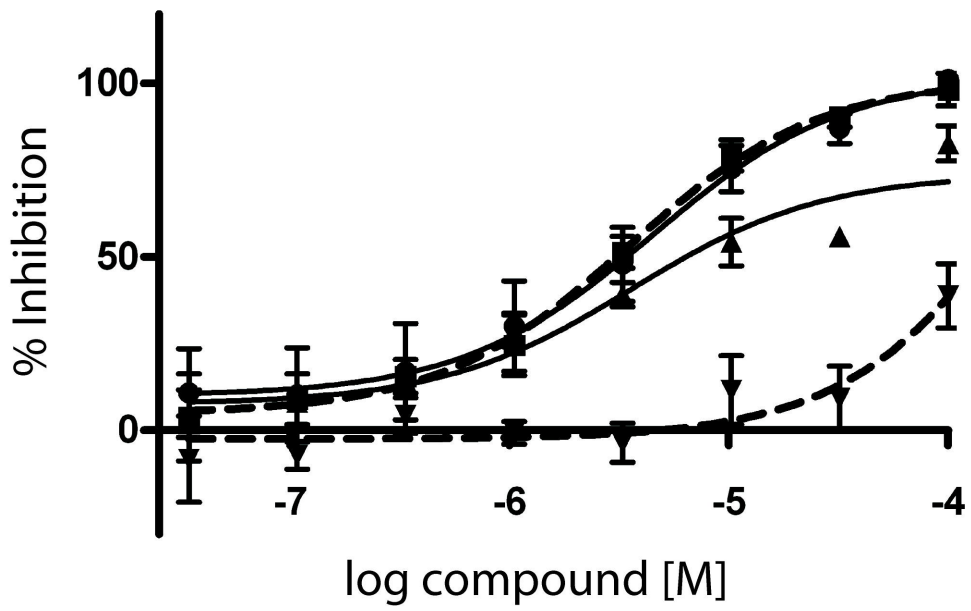


B

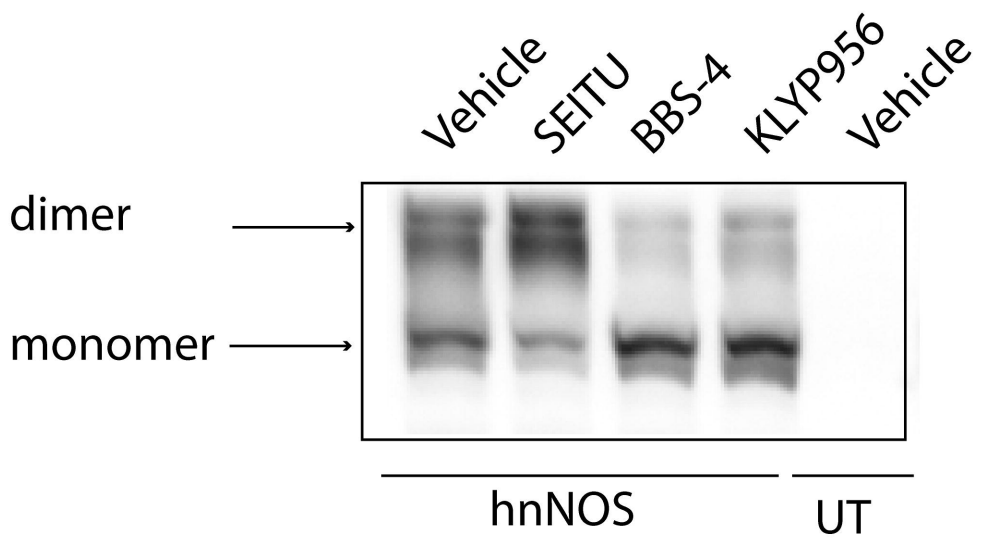




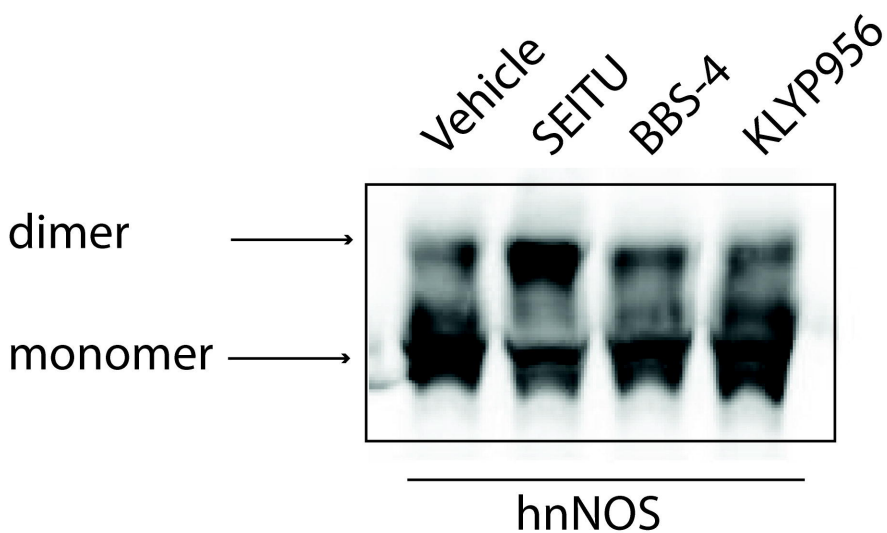
A



B



C



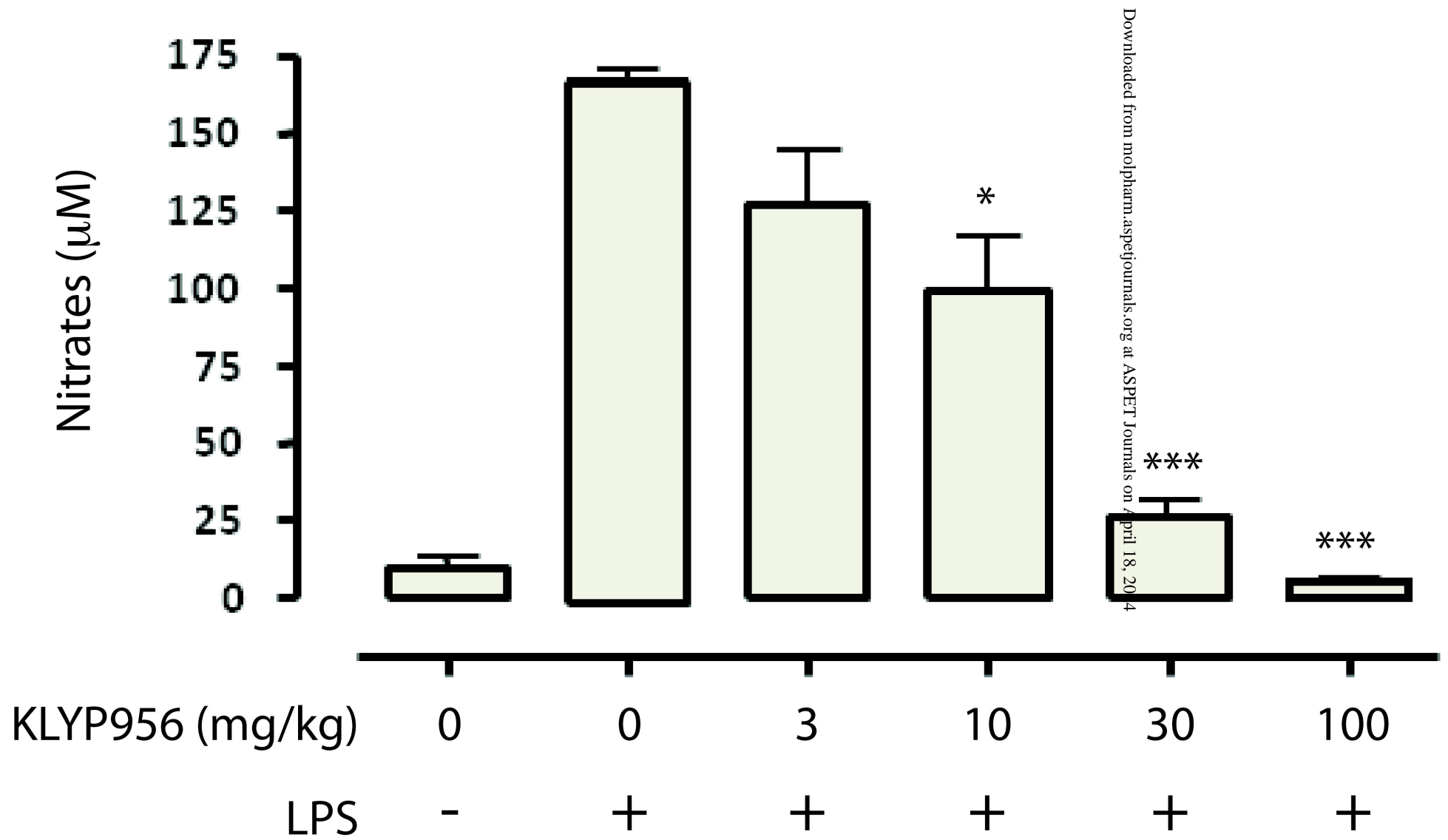
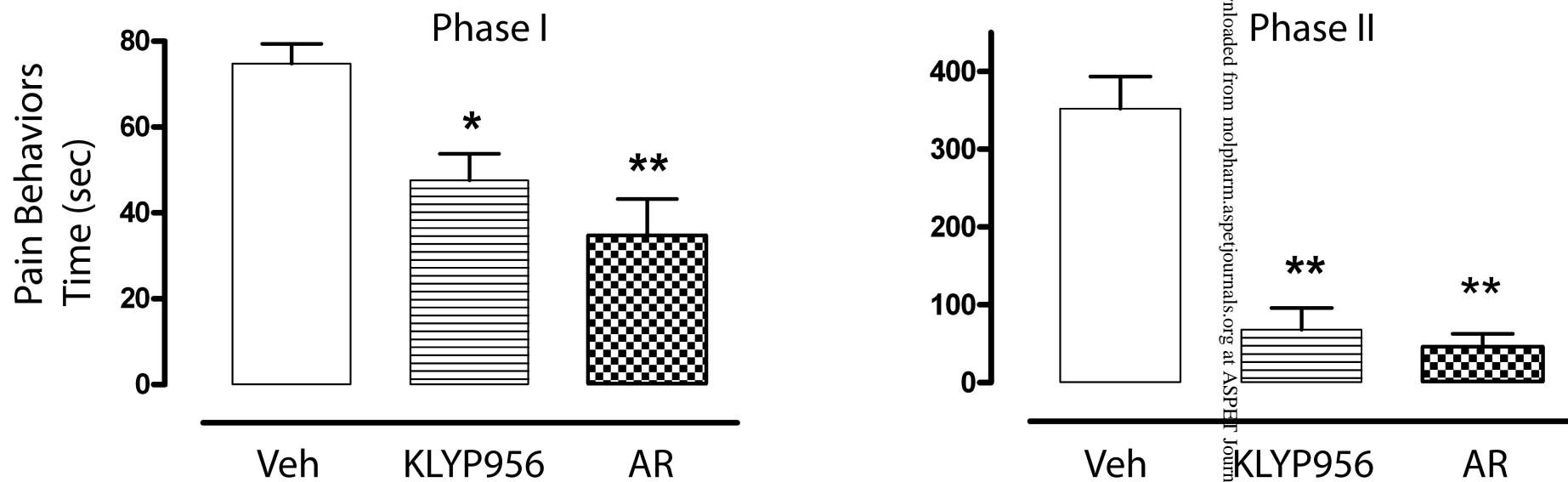


Figure 7

A



B

